Available online at www.sciencedirect.com
SCIENCE DIRECT®
ELSEVIER
Applied Surface Science 206 (2003) 271–293
applied surface science
www.elsevier.com/locate/apsusc

Surface viscoelasticity studies of Gd_2O_3, SiO_2 optical thin films and multilayers using force modulation and force–distance scanning probe microscopy

N.K. Sahoo*, S. Thakur, M. Senthilkumar, N.C. Das

Spectroscopy Division, Bhabha Atomic Research Centre, Trombay, Mumbai 400085, India

Received 21 August 2002; received in revised form 7 November 2002; accepted 7 November 2002

Abstract

The single and multilayer of Gd_2O_3 and SiO_2 thin films deposited through reactive electron beam evaporation have been studied for their viscoelasticity properties and optical spectral stability using multimode scanning probe microscope and spectrophotometric techniques. A conspicuous changes in viscoelasticity properties and surface topographies have been observed with the Gd_2O_3 films deposited under various oxygen pressures. The scanning probe measurements on the multilayer filters fabricated using these film materials for laser wavelengths of 248 nm (KrF) and 355 nm (Nd:Yag-III) have shown superior viscoelasticity property, which is not the case with the most conventional multilayers. The results were correlated with the long-term spectral stability that has been studied by recording transmittance spectra of these filters at a time interval of 10 months. Both the multilayer filters have shown excellent temporal spectral stabilities with a relatively better result for the 248 nm reflection filter. Further analysis has shown a very good co-relationship in the spectral stability and viscoelasticity properties in these multilayers.

PACS: 61.16.C; 42.79.W; 42.79.W; 78.20; 07.79; 78.66

Keywords: Surface viscoelasticity; Force modulation; Force–distance scanning probe microscopy

1. Introduction

Structural and spectral stabilities in multilayer optical coatings for various frontier technologies such as high power laser applications and optical communications have been a major concern over the years. Such application specific devices most often incorporate a large number of periodic or semi-periodic nano-layers of two or more different film materials to achieve varieties of spectral filtering functions [1]. Some of the most important considerations, which determine the technological success of these multilayer optical devices, are their microstructural and spectral stabilities over an appreciable time period after the development. It is well known that microstructural stability is very intimately associated with the spectral stability and has become the prime requirement of such precision optical thin film devices.

It is widely known that the optical coatings making use of single and multilayers of dielectric, metal and

* Corresponding author. Tel.: +91-22-2559-3871; fax: +91-22-2550-5151.
E-mail address: nksahoo@apsara.barc.ernet.in (N.K. Sahoo).

0169-4332/02/$ – see front matter
PII: S0169-4332(02)01233-3

ceramic films can produce varieties of spectral filtering functions to suit the requirements of several frontier optical technologies and experiments. The stability factor of such coatings becomes a critical issue, especially, for the coatings such as electric field optimized non-quarter-wave high damage threshold reflectors and DWDM filters using very large number of component layers [2]. It is well known that although one can achieve extremely good structural stability in single layer films, the same results deviate a lot while using the films in a multilayer structure incorporating other component layers. Invariably, the stability of a multilayer device falls far behind that of the individual single layers. The ultimate aim while designing and developing a multilayer optical coating is to achieve optical as well as microstructural stabilities at least compared to its component single layers.

Such stability considerations are not only essential for optical devices but also several other electronic and optoelectronic applications involving various heterostructures and superlattices. For example, alternating compressive and tensile strained layers in InGaAsP-based multiple quantum well structures are often designed to be strain balanced [3]. However, attaining a stable multilayer configuration is always a challenging task. There are several possible microscopic phenomena that can give rise to structural instability in multilayer devices and superlattices. For example, lateral strain modulations, surface modulation and interface undulations have been observed in strained heterostructures including III–V compounds as well as in SiGe/Si superlattices [4]. Lateral variations in surface morphology and alloy composition have been observed in unstable multilayer structures, which lead to degradation in optical properties [5]. Very interesting thickness modulations resulting into instabilities have also been observed in strained GaInAsP/(0 0 1)InP multilayers grown by gas source molecular beam epitaxy [6]. All these observations and investigations clearly highlight the importance of such stability studies relating to the multilayer structures.

2. Earlier studies on multilayer stability

The stability of lattice-mismatched thin films and multilayers has received a great deal of theoretical attention as well. A recently proposed mechanism suggests that elastic stresses induce morphological instabilities, which can lead to the formation of islands, non-planer surfaces, or in some cases the formation of deep, cusp-like morphologies [7–11]. Such morphologies can then provide sources for the nucleation of stress-reliving dislocations [11]. The wavelength of this type of instability is set by the competition between the stabilizing influence of thesurface energy and the destabilizing influence of the misfit-induced elastic strain energy. The case of multilayer films is significantly more complicated because it must include the effects of the relative magnitudes of the interlayer misfit strain and that imposed by the substrate in addition to the material (e.g. interfacial energies, elastic constants of multiple phases) and geometrical (i.e. layer thickness) parameters. It has been observed that the misfit between the layers in the film can destabilize the multilayer structure in cases where the thinner layer is elastically stiffer than the thicker layer [12]. By appropriate choice of the elastic moduli mismatch between the layers and relative layer thickness, the presence of an interlayer misfit can suppress the over all instability caused by the substrate misfit. The work of Sridhar et al. has shown that misfit stresses can destabilize a multilayer structure under conditions where interfacial diffusion is significant [12,13]. Even when there is no misfit between the layers, misfit between the multilayer structure and substrate can destabilize the interfaces and the over all structure.

The inherent compressive and tensile stresses of the component thin film layers are the main source of such structural instabilities in most multilayer optical coatings [13]. Various experimental studies have unequivocally indicated that instabilities occur both during growth and post-growth stages of these multilayer structures. Instabilities during the growth process, which are reflected in the process monitoring observables, can be controlled to some or large extent by optimizing the deposition parameters. However, post-growth instabilities are generated by accrued microstructural transformations influenced by the post-nucleation and environmental parameters. Such post-growth instabilities include morphological instabilities of the interfaces between the component layers (primarily for immiscible layers) or compositional modulations in miscible multilayer films. These

instabilities are now advantageously possible to investigate through a few advanced modes of atomic force microscopy (AFM). Surface viscoelasticity measurements using force modulation microscopy (FMM) and force–distance curve (FDC) measurements are a few of such advanced sensitive scanning probe techniques to explore the microstructural instabilities in single and multilayer structures. This FMM technique based on tip modulation and phase-sensitive detection, allows simultaneous recording of images of the surface profile, the storage modulus and the loss modulus of a sample. This ultimately identifies and maps the differences in surface stiffness (hardness) or elasticity, which is a representative of the structural stability of the single or multilayer thin film device.

2.1. Scope of the present study

Since the prime aim of our present research program is dedicated to optical applications of the thin film materials under study, all the theoretical and experimental analyses and interpretations in this paper have been confined to this particular direction only. Moreover, the spectral characteristics of an optical multilayer device indirectly represent several other important aspects of the microstructure and stress related information that is strongly correlated with the dielectric properties of the component thin film layers. In this work, several single and multilayer optical coatings using gadolinium oxide (Gd_2O_3) and silicon dioxide (SiO_2) have been investigated for their structural and spectral stabilities using the viscoelastic imaging results of the force modulation and force versus distance measurements through AFM and spectrophotometric transmittance measurements. The surface topographies of these films have also been analyzed to correlate these measurements with the structural stability. These refractory oxide films have been identified to be the most favorable candidates in developing precision multilayer coatings for lasers, spectroscopy, optical communication and several other applications pertaining to these pioneering fields, especially in the ultraviolet (UV) and deep ultraviolet (DUV) region (0.2–0.35 mm) of the electromagnetic spectrum.

Although SiO_2 is a very familiar material for the optical coating applications, Gd_2O_3 is very new to the optical coating material family. This novel Gd_2O_3 thin film material has a very special property of wide spectral transmission, which extends from deep ultraviolet to infrared (0.2–16 μm) [14]. It is well known that the ultraviolet region from 0.2 to 0.35 μm is a very important region of the electromagnetic spectrum, which represents state-of-the-art in both lasers and coatings. Most of the refractory oxide coating materials, which are transparent in the visible, become highly absorbing in this UV region due to band gap absorptions. Thus, this spectral region has been posing considerable challenges with respect to UV-transmitting thin film materials and their appropriate combinations. The novel gadolinium oxide with its high band gap value of >6.35 eV has become a very promising candidate for making optical filters for ultraviolet and deep ultraviolet region of the electromagnetic spectrum. Also it can form very durable films under lower even at ambient substrate temperatures, which makes it an attractive candidate for varieties of substrate and film material. However, an important consideration, which determines the technological success of these materials, is their microstructural and corresponding spectral stability. Long-term spectral stabilities of the two different multilayer optical reflecting filters, developed for KrF (248 nm) and Nd:Yag-III (355 nm) laser wavelengths using these two film materials, have been compared with these microstructural measurements.

The long-term structural stability has been closely monitored by measuring the spectral stability of these reflectors using an UV-Vis-NIR spectrophotometer (model: Shimadzu UV2301PC) with a substantial time-gap of 10 months. Both the multilayer filters have shown extremely stable spectral as well as structural properties. However, the 25-layer reflecting filter developed for KrF (248 nm) laser applications showed relatively better spectral stability with respect to 21-layer reflector developed for Nd:Yag-III (355 nm) wavelength. The possible explanation for this better performance can be attributed to the effect of additional number of layers in the multilayer structure that might have contributed to the overall strain compensation. The results of this measurement can be very well visualized through the viscoelastic and force–distance measurements carried out on these multilayers.

3. Force modulation measurements

In advanced atomic force microscopy, in addition to the topographic feature, one can probe local elastic (stiffness) properties of materials through a mechanical interaction between the surface and the tip [15]. In standard contact mode AFM, the probe is scanned over the surface (or the sample is scanned under the probe) in an x–y raster pattern. The feedback loop maintains a constant cantilever deflection, and consequently a constant force on the sample. With the force modulation technique, the probe also moves with a small vertical (z) oscillation (modulation), which is significantly faster than the scan rate. The force on the sample is modulated about the set-point scanning force such that the average force on the sample remains equal to that in simple contact mode. When the probe is modulated into contact with a sample, the sample surface resists the oscillation and the cantilever bends. Under the same applied force, a stiff area on the sample will deform less than a soft area; i.e. stiffer areas put up greater resistance to the vertical oscillation and, consequently, greater bending of the cantilever. The variation in cantilever deflection amplitude at the frequency of modulation is a measure of the relative stiffness of the surface. Topographical information (dc, or non-oscillatory deflection) is collected simultaneously with the force modulation data (ac, or oscillatory deflection). Elasticity difference on a surface can be distinguished by using this technique. It is clear that such a technique works well when measuring the slope of the force–distance curves at the repulsive force region. Early designs for this technique add a modulation signal to the z-section of the piezoelectric scanner to induce the vertical oscillation. While this technique has been somewhat successful and widely duplicated, it has some drawbacks. The additional high-frequency modulation signal can excite any of a number of the scanner's mechanical resonances. This unwanted crosstalk can reduce the quality of both the topographic and the force modulation images. This approach has been very much refined in the advanced SPM instruments. Such instruments, like our present system use a second-generation force modulation system that contains an additional piezoelectric actuator to separately modulate the tip (cantilever) position. This actuator can reduce or eliminate spurious excitation of scanner resonances. The actuator is generally driven at frequencies of approximately 5–20 kHz for force modulation experiments. Combined with advanced interleaved scanning, these advanced force modulation tip holders provide a wide range of new capabilities. The modulation signal is generated with a high-precision digital frequency synthesizer with advanced software functionality that allows the user to quickly select an optimum modulation amplitude and frequency. The cantilever oscillation amplitude is measured with a high-speed phase-sensitive detection circuitry providing a noise level of <1 Å over a bandwidth greater than 1 MHz. The result is a technique with superior discrimination of sample stiffness and minimal susceptibility to topographic artifacts. In these cases, the cantilever deflection Δz can be related to the force modulation ΔF acting on the tip by $\Delta F = k\,\Delta z$, where k is the cantilever spring constant.

4. Force–distance measurements

With force versus distance curves, AFM can distinguish surface regions of different stiffness (hardness) and adhesion characteristics [16]. Besides, such measurements also very precisely give the viscoelastic responses of the surface. In this technique, briefly, forces applied on the surface are measured by the deflection of the cantilever while approaching and retracting from the surface. A typical force distance curve is shown in the Fig. 1. Qualitatively, the steeper the slope, the stiffer (harder) is the sample. An inverted peak, seen in the middle of the force versus distance curve (Fig. 1), during retraction of the cantilever indicates some adhesion between the tip and the sample. The force versus distance curve not only shows the difference qualitatively, but also permits quantitative measurement of the adhesion force through suitable modeling and analysis techniques.

5. Statistical analysis

As mentioned earlier, the surface topography of multilayer film considerably differs from its component individual single layer films. The surface topographic comparison between the individual component layers

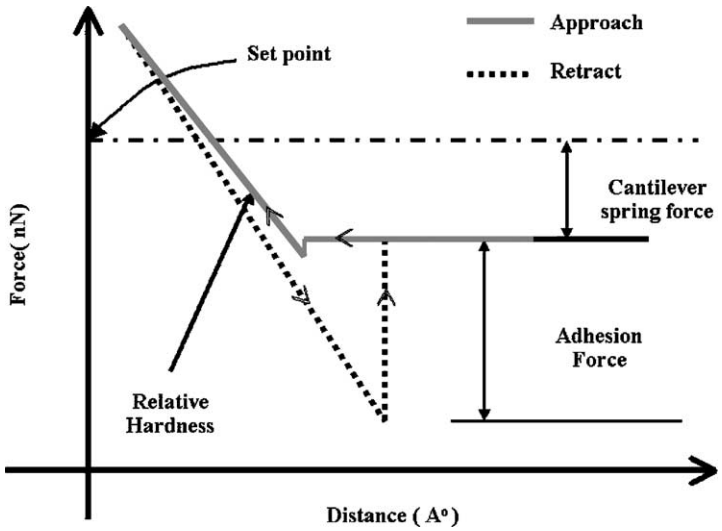

Fig. 1. A typical force vs. distance curve depicting force on the cantilever during the approach and retract process during an AFM measurement.

and the multilayer gives an idea of the structural stability and its component layer's compatibility. The surface topographic statistical analysis of the single and multilayer thin films can also be correlated with elasticity measurements obtained from the force modulation and force–distance measurements. Statistical analyses were carried out for all the acquired data so that their process dependent changes can be

Table 1
Surface statistics of single layer films (Gd_2O_3 thin film samples)

Sample no.	Process parameters			Surface statistics from the AFM measurements					
	Rate (nm/s)	Substrate temperature (°C)	Oxygen pressure (mbar)	R_{max} (nm)	R_{mean} (nm)	R_a (nm)	R_q (nm)	R_{sk} (nm)	R_{ku} (nm)
1	1.0	70	0.5×10^{-4}	189.99	52.91	17.2	24.832	1.548	6.201
2	1.0	70	0.8×10^{-4}	135.2	19.4	4.249	6.895	4.894	56.084
3	1.0	70	1.0×10^{-4}	168.48	43.329	20.09	27.76	1.31	4.043
4	1.0	70	2.0×10^{-4}	154.83	20.331	4.809	9.588	4.021	35.574

Table 2
Surface statistics of multilayer reflectors ($Gd_2O_3 + SiO_2$ thin film multilayers)

Sample type	Process parameters			Multilayer surface statistics from the AFM measurements					
	Rate (nm/s)	Substrate temperature (°C)	Oxygen pressure (mbar)	R_{max} (nm)	R_{mean} (nm)	R_a (nm)	R_q (nm)	R_{sk} (nm)	R_{ku} (nm)
248 nm (KrF laser) Reflection filter (25-layer)	Gd_2O_3:1.0 SiO_2:2.0	70 70	0.8×10^{-4} 1.0×10^{-4}	83.655	42.448	2.230	3.945	4.628	54.321
355 nm (Nd:Yag-III) Reflection filter (21-layer)	Gd_2O_3:1.0 SiO_2:2.0	70 70	0.8×10^{-4} 1.0×10^{-4}	49.595	15.757	3.054	4.545	2.213	11.482

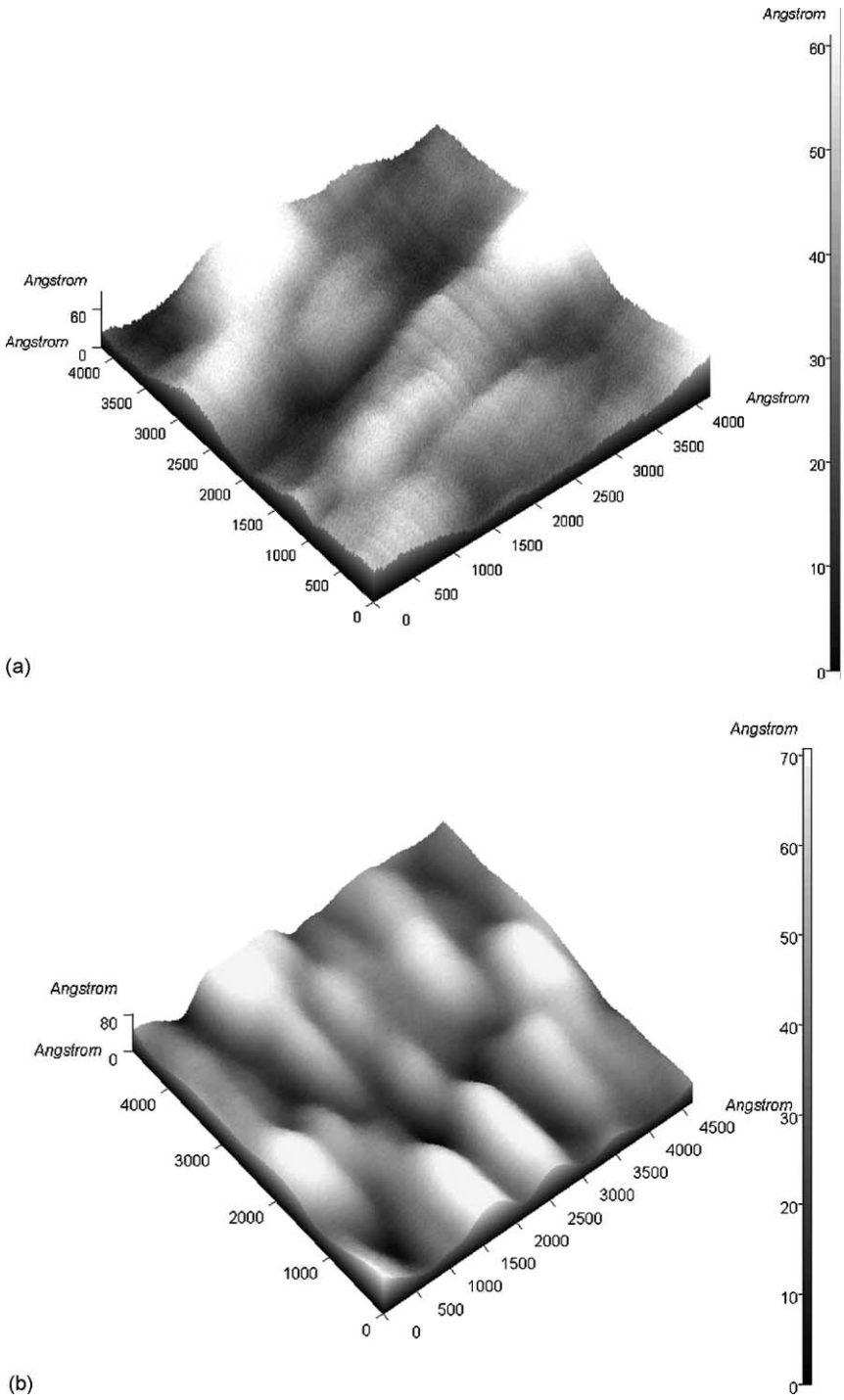

Fig. 2. AFM surface topographic images of gadolinium oxide thin films deposited under oxygen pressures of (a) 0.5×10^{-4} mbar, (b) 0.8×10^{-4} mbar, (c) 1.0×10^{-4} mbar and (d) 2.0×10^{-4} mbar.

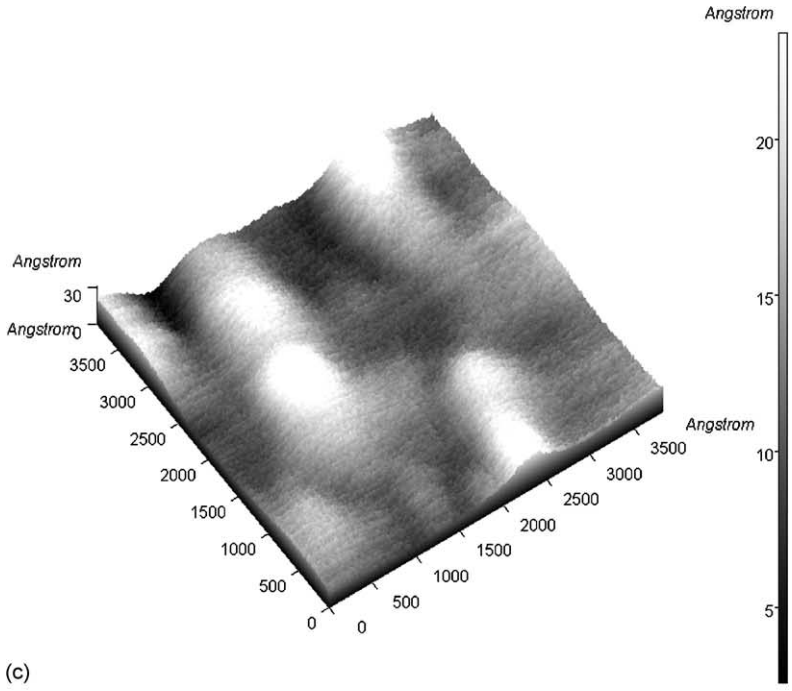

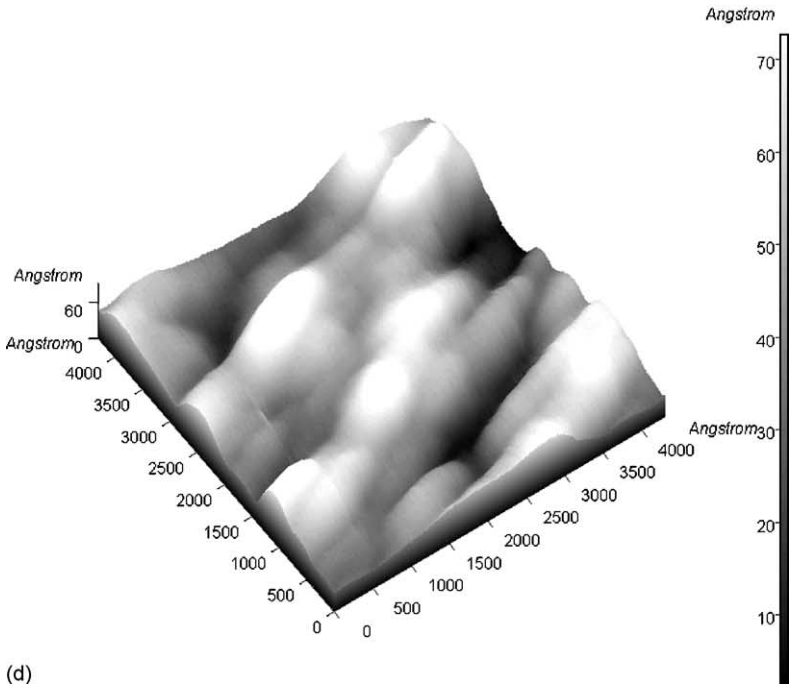

Fig. 2. (*Continued*).

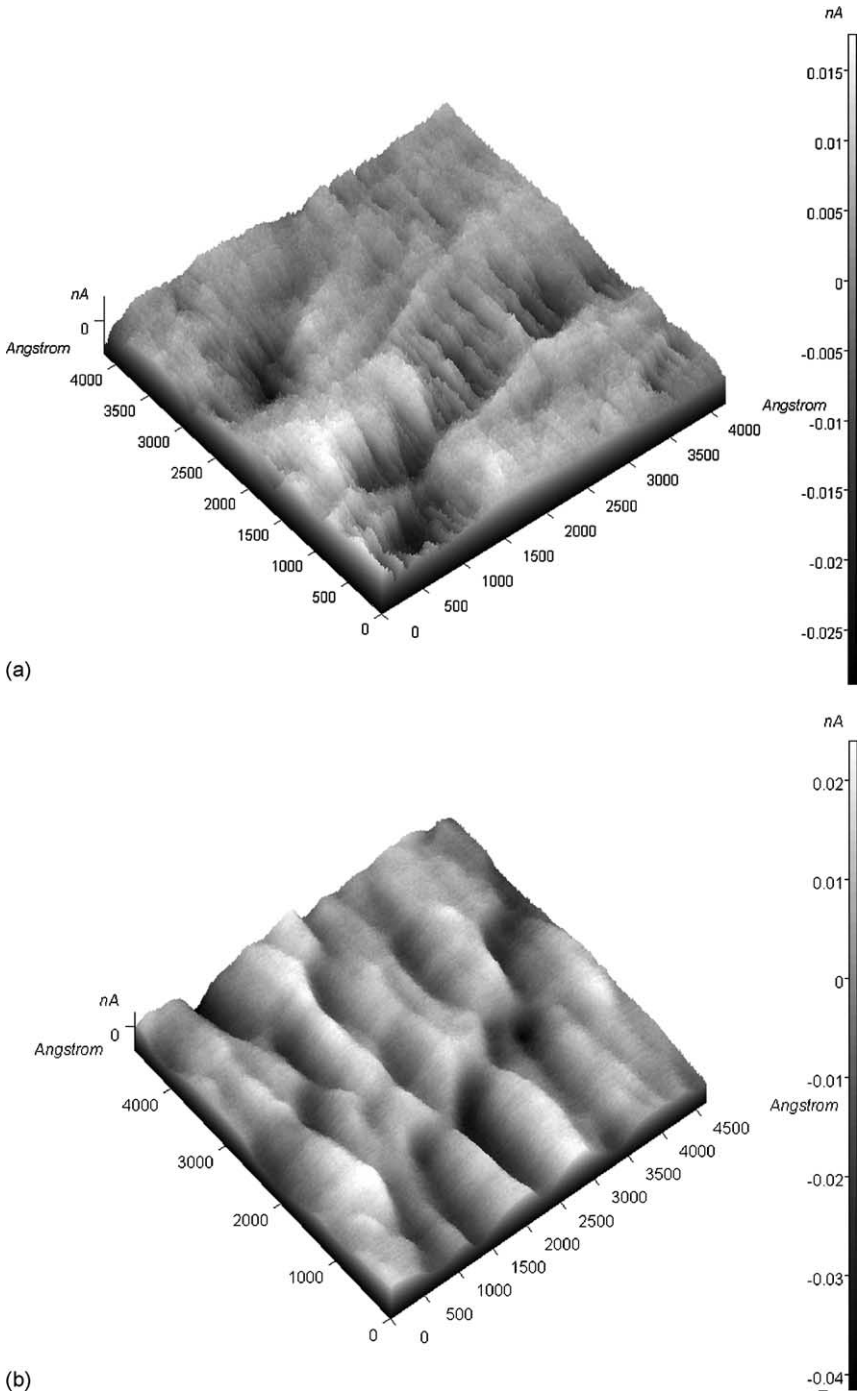

Fig. 3. Force modulation (viscoelasticity) images of gadolinium oxide thin films prepared at oxygen pressures of: (a) 0.5×10^{-4} mbar, (b) 0.8×10^{-4} mbar, (c) 1.0×10^{-4} mbar and (d) 2.0×10^{-4} mbar.

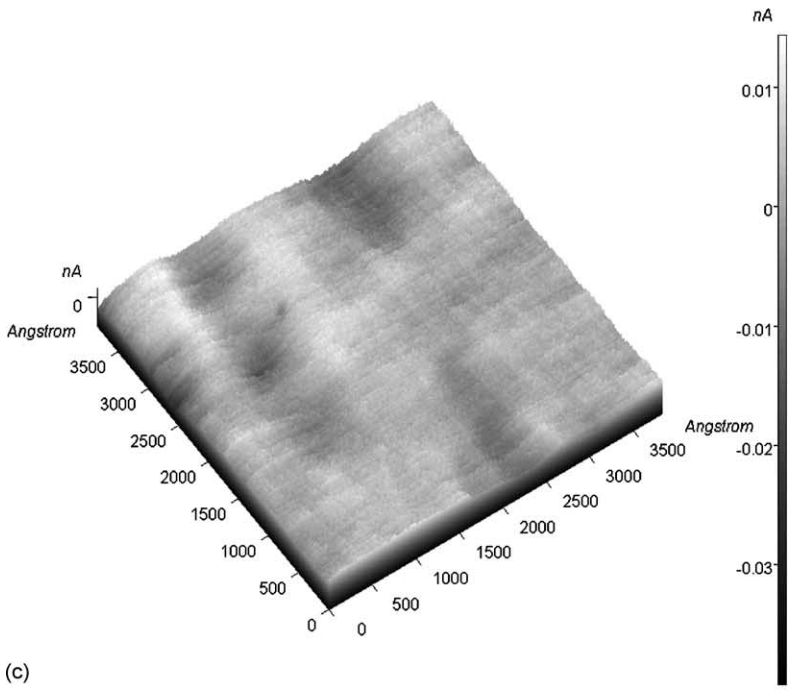

(c)

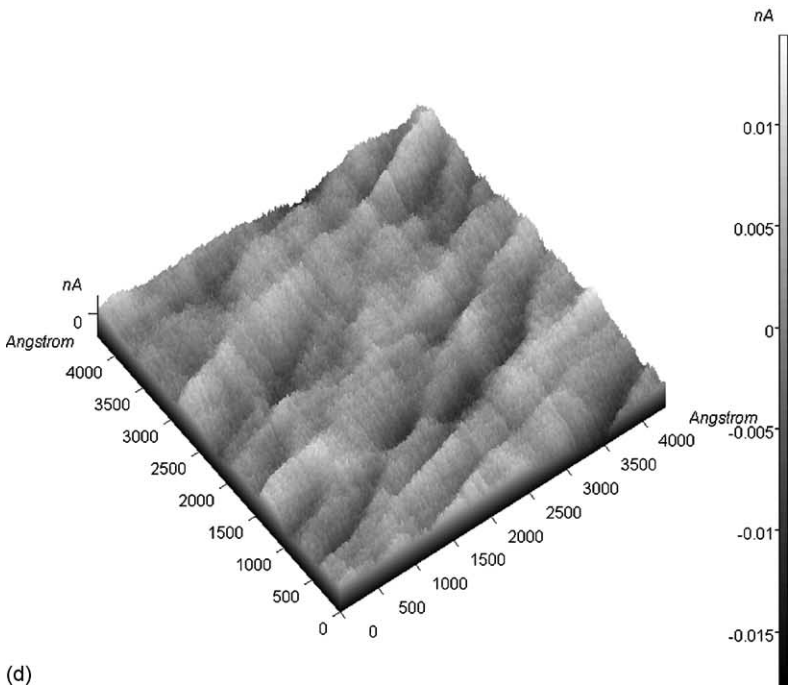

(d)

Fig. 3. (*Continued*).

assessed and correlated. The following statistical parameters are of interest with respect to the present experiments:

R_{max}: This parameter defines the difference between maximum and minimum values of Z-coordinate (Z_{max}, Z_{min}) on the surface within the analysis area (i.e. height drop) and is given by

$$R_{max} = Z_{max} - Z_{min} \tag{1}$$

R_{mean}: It defines the Z-coordinate average value on the sample surface within the analysis area and is given by

$$R_{mean} \equiv Z_{mean} = \frac{1}{N_x N_y} \sum_{i=1}^{N_x} \sum_{j=1}^{N_y} Z_{ij}, \quad Z = Z_{ij} - R_{mean} \tag{2}$$

where N_x, N_y are the number of points in x- and y-direction of the scanned image. Z_{max} and Z_{min} are the maximum and minimum values of the topography recorded during the measurement.

R_a: It defines the average value of the surface roughness within the area being analyzed

$$R_a = \frac{1}{N_x N_y} \sum_{i=1}^{N_x} \sum_{j=1}^{N_y} |Z(i,j) - Z_{mean}| \tag{3}$$

R_q: It defines the standard deviation for Z-coordinate on the sample surface within the area being analyzed

$$R_q = \sqrt{\frac{1}{N_x N_y} \sum_{i=1}^{N_x} \sum_{j=1}^{N_y} (Z(i,j) - Z_{mean})^2} \tag{4}$$

R_{sk} (skewness): It defines the asymmetry value in the sample surface within the area being analyzed

$$R_{sk} = \frac{1}{N_x N_y R_q^3} \sum_{i=1}^{N_x} \sum_{j=1}^{N_y} (Z(i,j) - Z_{mean})^3 \tag{5}$$

R_{ku} (kurtosis): It defines the sample surface excess with the area being analyzed:

$$R_{ku} = \frac{1}{N_x N_y R_q^4} \sum_{i=1}^{N_x} \sum_{j=1}^{N_y} (Z(i,j) - Z_{mean})^4 \tag{6}$$

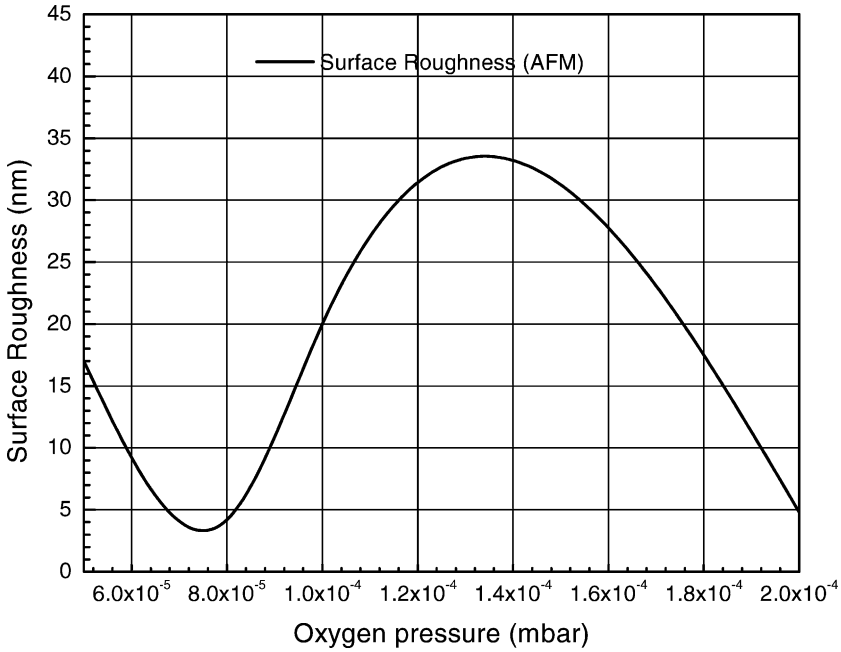

Fig. 4. Variation of surface roughness of Gd_2O_3 thin films measured through AFM measurements with respect to various oxygen pressures.

The measured statistical values of various single and multilayer thin film samples are presented in Tables 1 and 2.

6. Results and analysis

In the present work, two different optical dielectric film materials namely Gd_2O_3 and SiO_2 have been studied for their viscoelasticity properties both as single and multilayers. Along with the viscoelastic studies, surface statistical analyses were carried out for each sample film simultaneously to observe and correlate the process parametric influences on the surface topographies and viscoelasticity. Out of these two film materials, the novel Gd_2O_3 has a several superior properties both spectrally and structurally. The following sections describe the experimental results on the individual films and the multilayers.

6.1. Gd_2O_3 single layer films

For the present investigations, gadolinium films have been prepared by reactive electron beam deposition process in a fully automated optical coating unit—VERA-902. The gadolinium oxide granules of Cerac's product-G-1076 with the purity >99.9% have been used for this thin film preparation. The real time rate of deposition and total physical thickness were controlled and determined by Leybold's XTC/2 quartz crystal monitors. A residual gas analyzer of Pffeier's Prisma-200 has been used to analyze the partial pressure of reacting gases. Leybold's OMS-2000 optical monitoring system has been used to record the optical thickness using quarter-wave monitoring approach. For controlling the total pressure during the reactive evaporation process, MKS mass flow controllers have been suitably interfaced with the coating system. Various thin film samples with different process parameters have been prepared for the present investigation. The special aim in this study was to investigate the oxygen enrichment effect on the spectral and microstructural properties of Gd_2O_3 films. The oxygen partial pressure has been varied in our experiment from 0.5×10^{-4} to 2×10^{-4} mbar. The substrate temperature and rate of deposition were kept at 70 °C and 10 Å/s, respectively, in order to have a suitable matching property with SiO_2.

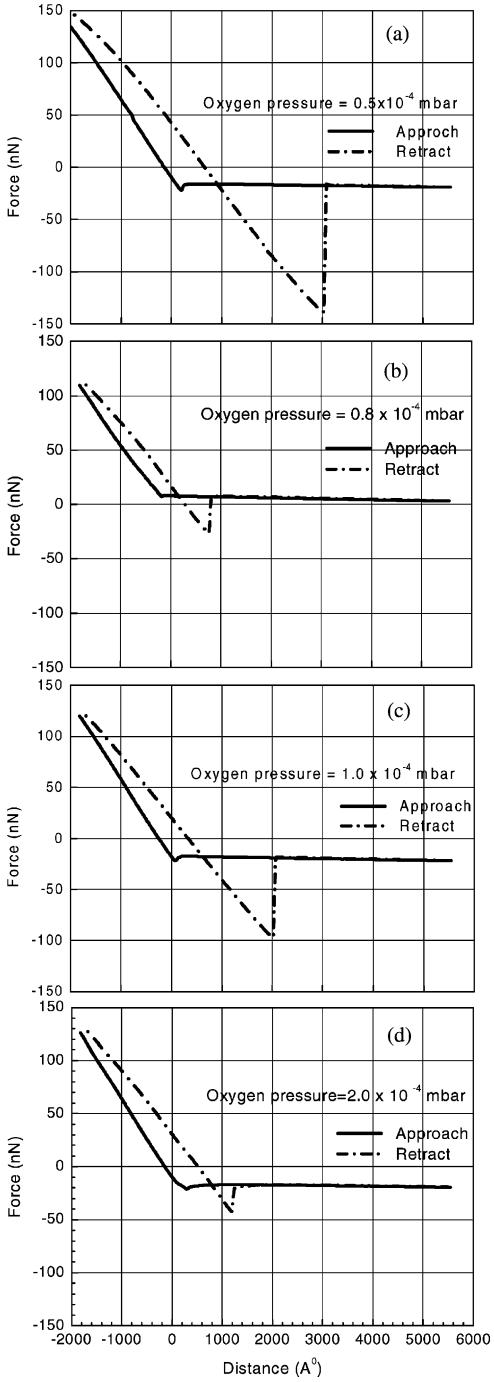

Fig. 5. Plots of force vs. distance curves at oxygen pressures values of (a) 0.5×10^{-4} mbar, (b) 0.8×10^{-4} mbar, (c) 1.0×10^{-4} mbar and (d) 2.0×10^{-4} mbar.

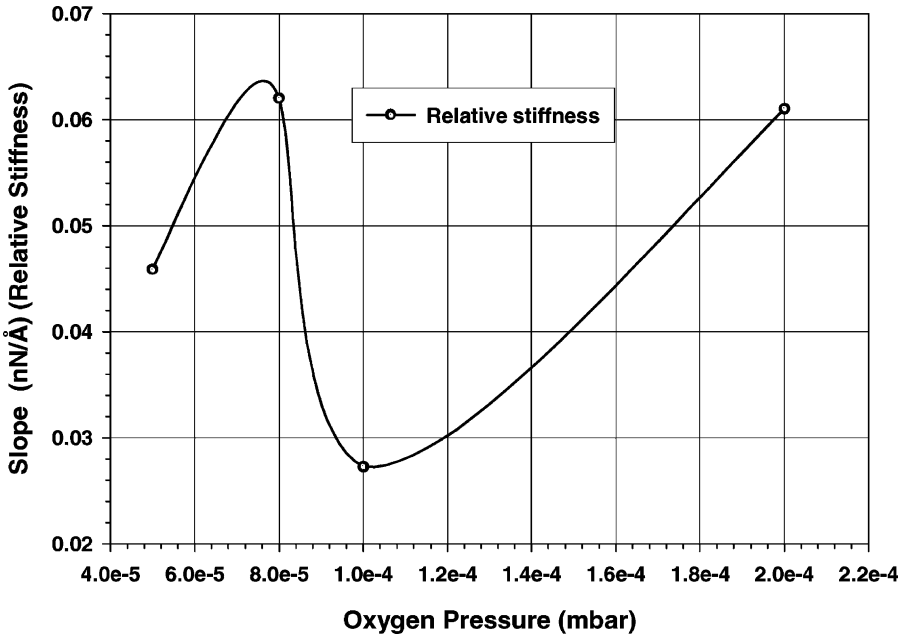

Fig. 6. Variation of relative stiffness derived from the slope values of force vs. distance curves at different oxygen partial pressures.

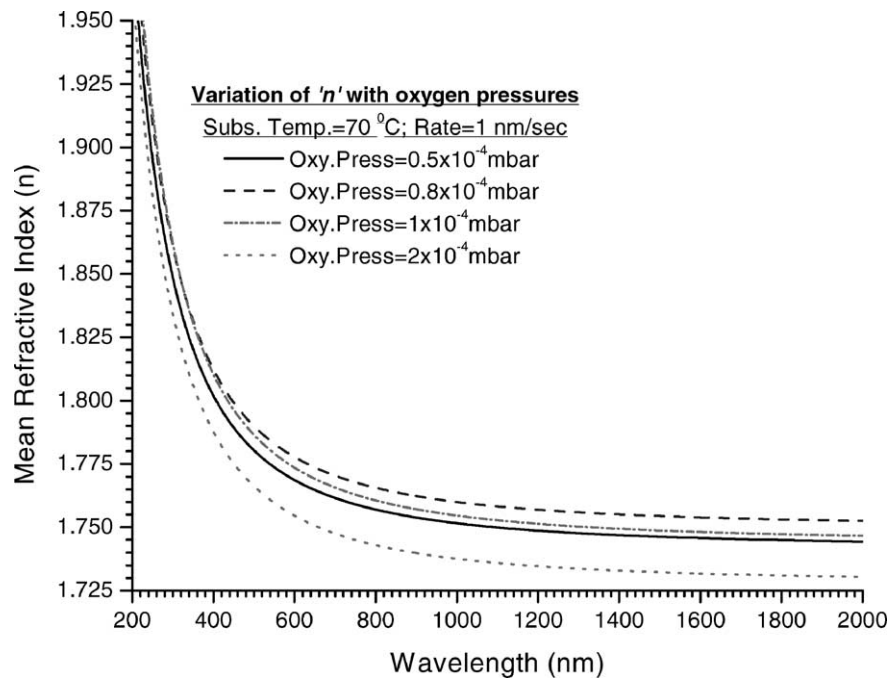

Fig. 7. Variation of spectral refractive index (n) profile for Gd_2O_3 films deposited under various oxygen pressures of 0.5×10^{-4} mbar, 0.8×10^{-4} mbar, 1.0×10^{-4} mbar and 2.0×10^{-4} mbar.

NT-MDT's Solver P-47H Multimode scanning probe microscope system has been employed to acquire and analyze the surface topographies, force modulation and force versus distance curve measurements of these single layer Gd_2O_3 thin films. The cantilever having low spring constant of 0.6 N/m and resonance frequency of 75 kHz has been chosen to get good topographic and force modulation images. During the measurements, the scanning parameters such as scanning speed and feedback gain values have been scrupulously selected to acquire the optimum quality AFM images.

Fig. 2a–d portrays the surface topographic images of single layer Gd_2O_3 thin films deposited at four different oxygen partial pressures. Fig. 3a–d depicts the corresponding force modulation Images. It is evident from these figures that for these sample films the force modulation images have a strong co-relationships with the topographic features. The surface topographies of these films were also analyzed to extract the surface statistical information. The details of the surface topographic results are presented in the Table 1. It can be observed from Table 1 that at a substrate temperature of 70 °C, the oxygen partial pressure of 0.8×10^{-4} mbar gives the lowest roughness value (R_{mean}). Fig. 4 portrays the variation of surface roughness with respect to oxygen pressure. The thin film deposited at oxygen pressures of 0.8×10^{-4} and higher oxygen pressures have yielded smooth surface topographies.

The force versus distance curves has also been measured to investigate the structural stability. Fig. 5a–d depict the force versus distance curves measured for thin films deposited under various oxygen pressures. In viscoelasticity measurements, the slope of the curve is a representative of the stiffness (hardness) of the material. The steep slope for the sample film prepared under oxygen pressure 0.8×10^{-4} mbar (Fig. 5b) entails its superior stiffness property over other samples. Fig. 6 portrays the variation of slope with respect to oxygen partial pressure. The data are spline fitted in order to visualize a smooth functional behavior. The sample films prepared under oxygen pressures of 0.8×10^{-4} and 2.0×10^{-4} mbar exhibited higher slopes, which is a representative of their superior stiffness. But the refractive index measurements have shown a superior value for the sample prepared under the oxygen

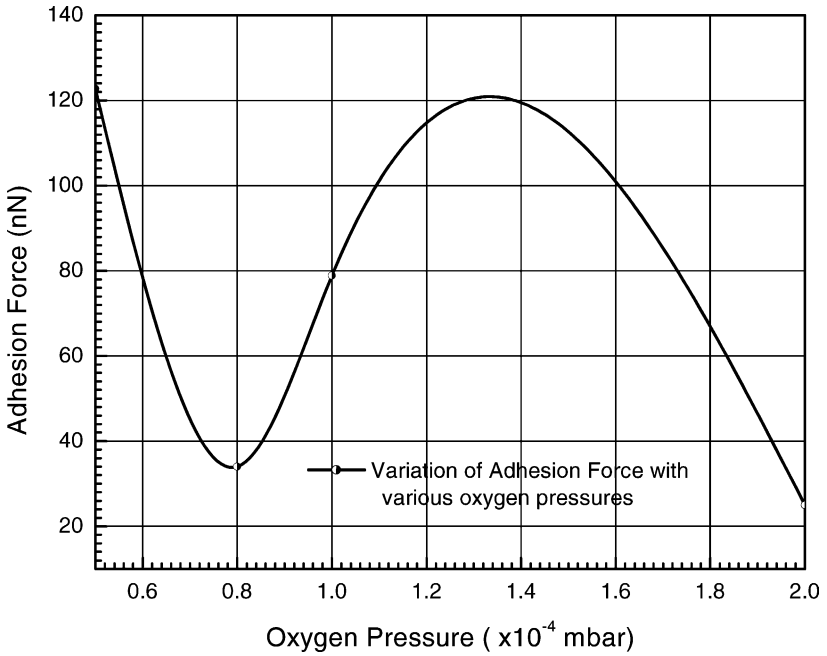

Fig. 8. Plot depicting variation of adhesion force with respect to various oxygen pressures.

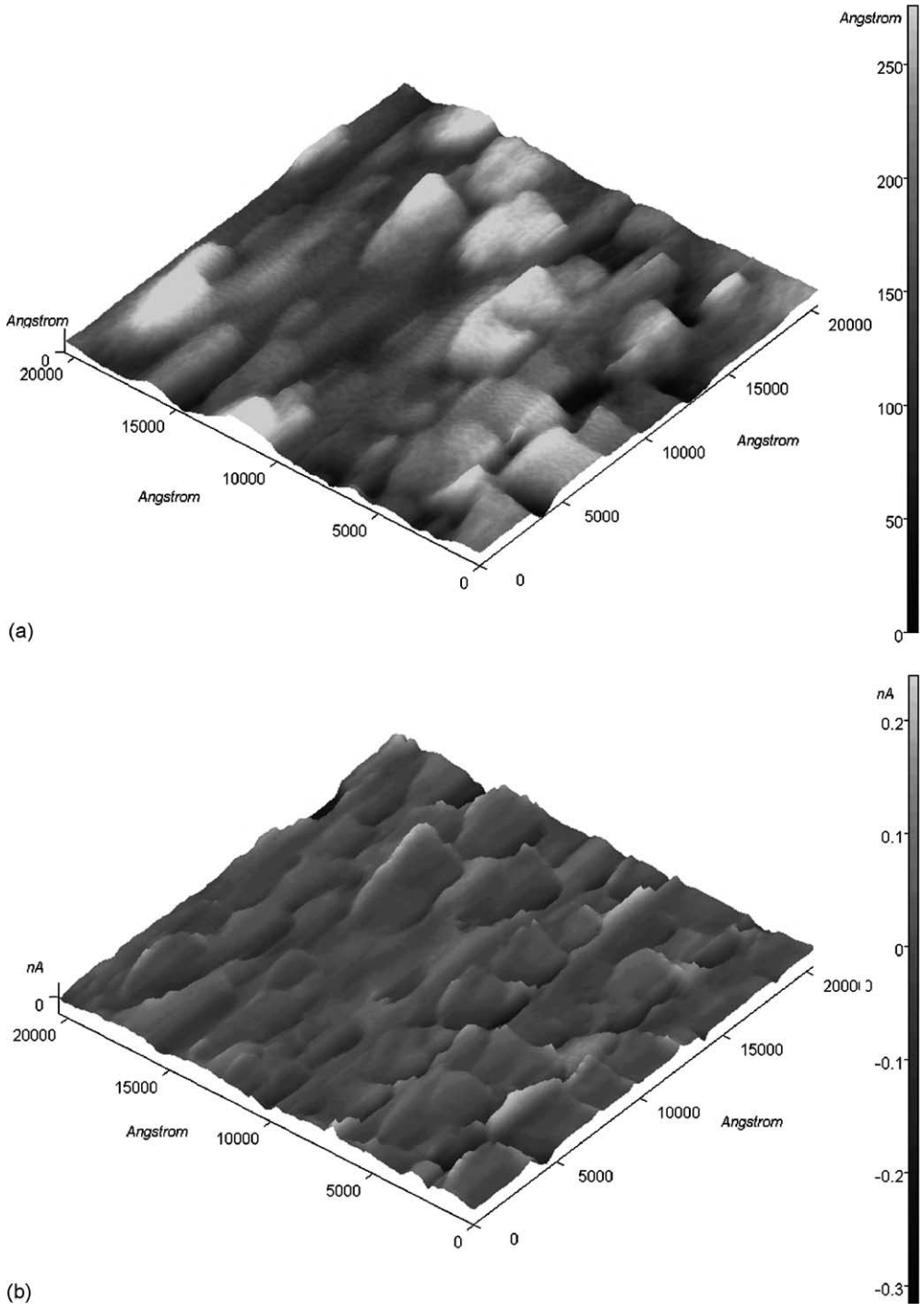

Fig. 9. (a) Surface topography and (b) force modulation images of single layer SiO_2 thin film.

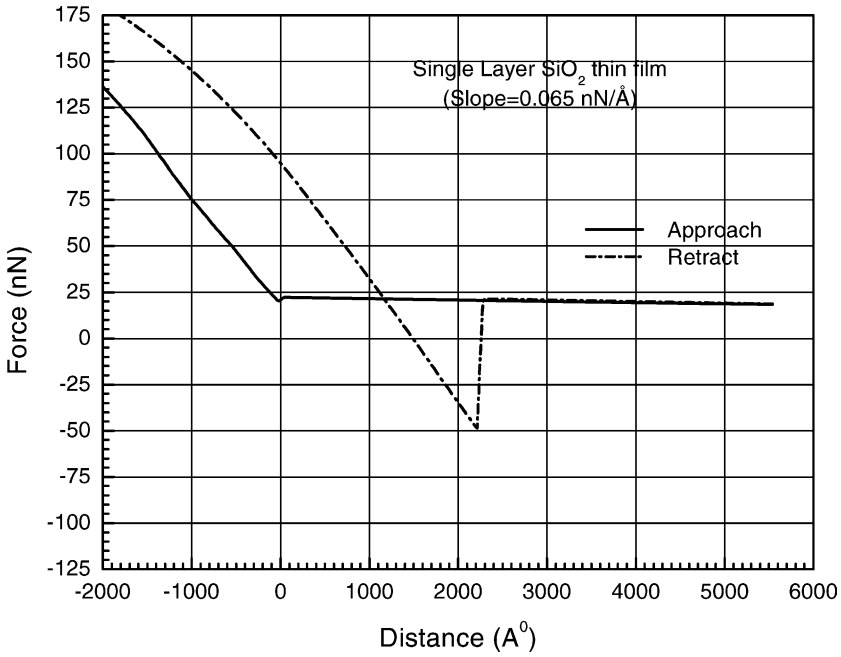

Fig. 10. Force vs. distance curve for the single layer SiO_2 thin films.

pressure of 0.8×10^{-4} mbar and is depicted in the Fig. 7.

As mentioned earlier, the amplitude of the inverted peak appeared in the force versus distance curve (Fig. 1) that represents the adhesion force. The computed adhesion force from the force versus distance curve with respect to various oxygen pressures is portrayed in Fig. 8. At 0.8×10^{-4} and 2.0×10^{-4} mbar pressures, the Gd_2O_3 films exhibit lower adhesion force compared to thin films deposited under other oxygen pressures. Interestingly, films with higher values in adhesion force exhibits small relative stiffness and the vice versa.

6.2. SiO_2 single layer films

Silicon dioxide is the most popular and widely used well-behaved optical coating material in the field of optical coating. It is best known for its low refractive index and superior compatibility with several refractory oxides for developing multilayers filters and devices. For the present experiments, a few samples of SiO_2 films have been prepared at optimized conditions in the above deposition system. Substrate temperature values of 70 °C and oxygen pressure of 1×10^{-4} mbar were chosen for an optimum compatibility with Gd_2O_3 films in developing the multilayer filters. Surface topography and force modulation images of single layer SiO_2 thin film are shown in Fig. 9a and b. To study the stiffness and adhesion force, a force versus distance measurement has been carried out with the single layer thin film, which is depicted in Fig. 10. The measured adhesion force and slope values are 70.02 nN and 0.065 nN/Å, respectively. Such a slope value is a close match with that of Gd_2O_3 films deposited under oxygen pressure of 0.8×10^{-4} mbar. For developing multilayer coatings, such a combination was chosen to establish a stable configuration.

6.3. Multilayer devices using Gd_2O_3 and SiO_2 component films

Two different multilayer reflection filters have been made using Gd_2O_3 as high index and SiO_2 as low index component layer. The optimized process parameters were chosen to achieve a similar stiffness values in the component film materials. As discussed earlier, the optimized process conditions for SiO_2 and

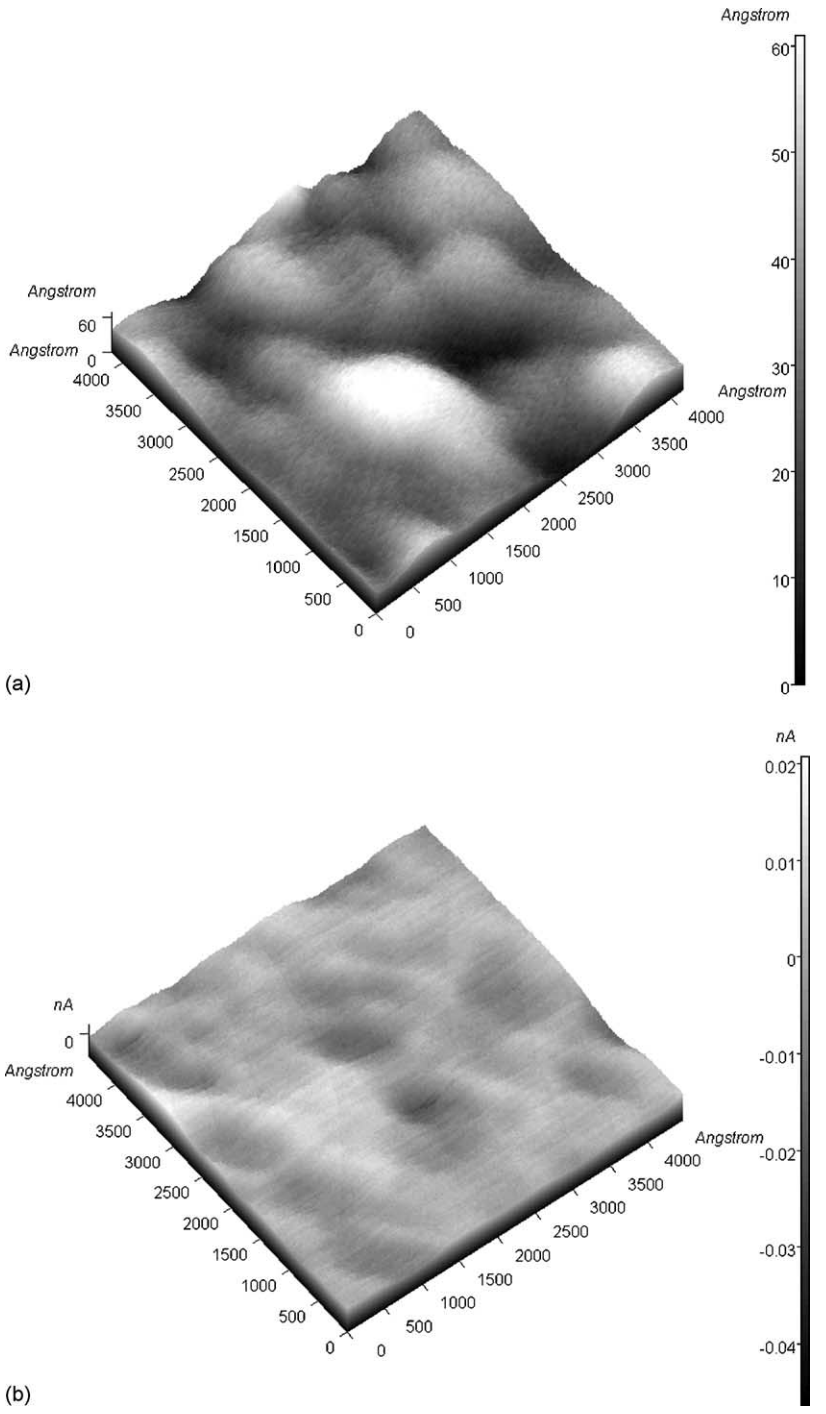

Fig. 11. (a) Surface topography and (b) force modulation image of 25 alternate layers of Gd_2O_3 and SiO_2 248 nm reflection filter for KrF laser recorded just after the development (October 2001).

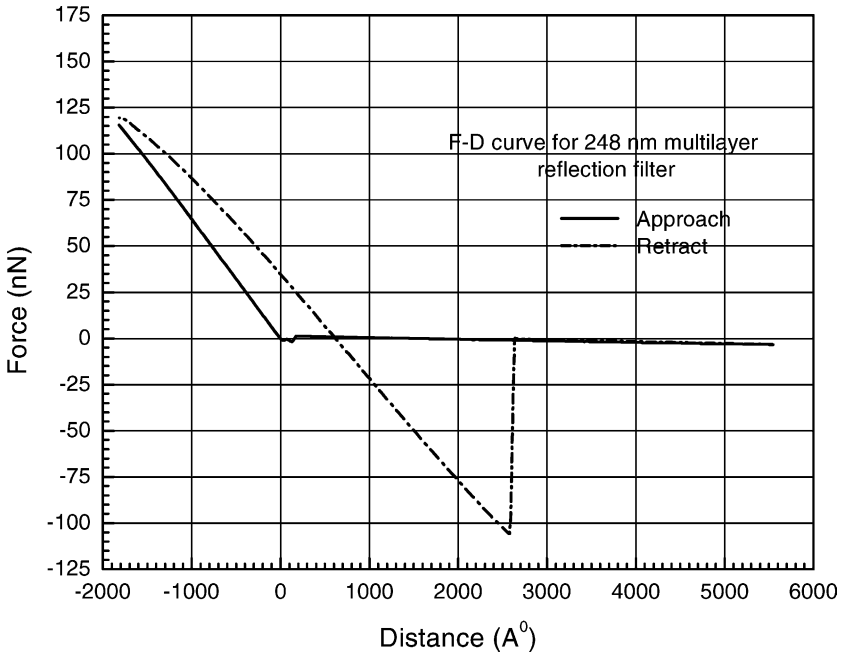

Fig. 12. Force vs. distance curve for the 25-layer 248 nm reflection filter.

Gd_2O_3 films have shown the slope values (stiffness) of 0.065 and 0.064, respectively. Such a good match in the stiffness has ultimately resulted into a stable multilayer structure as can be seen in the subsequent section. Advantageously, Gd_2O_3 films have also shown higher refractive index values at these optimized process parameters which is an essential criterion for the multilayer development task.

The developed multilayer filter devices were meant for some spectroscopic experiments being carried out in our laboratory using Nd:Yag-III and KrF lasers which have lasing wavelengths at 355 and 248 nm, respectively. The higher band gap of >6.35 eV in optimized Gd_2O_3 films has made it suitable to make multilayer coatings in deep ultraviolet region such as KrF (248 nm) laser wavelength. As discussed earlier, the stability factor in the component films changes when it forms a multilayer by combining with other materials. To probe the structural stability of our present multilayer devices; surface topography, force modulation and force versus distance measurements have been appropriately carried out. Fig. 11a and b depicts the measured surface topography and corresponding force modulation images of 248 nm reflection filter. The multilayer's topography shows a relatively improved grain structure. The details of the surface statistics of this multilayer have been shown in the Table 2. It can be seen from this table that the surface topography of this multilayer is better than its individual component layers. This indicates that the microstructure of the final multilayer has been improved by choosing the component layers deposited under optimized process parameters. Fig. 11b portrays corresponding force modulation image, which is also very smooth indicating a uniform elasticity all over the film. Fig. 12 depicts force versus distance curve obtained on this multilayer, which indicates good adhesion and stiffness that is not the case with most conventional optical multilayers. The adhesion force and the slope values (relative stiffness) are 106 nN and 0.0564 nN/Å, respectively, which are better than the component layers. Fig. 13a shows the surface topography of 355 nm reflection filter. This topography image also shows the fine grains structure over its component layers. The surface statistics information of the multilayer is presented in Table 2. It can be noticed from this table that roughness value for this multilayer is lower than the individual component

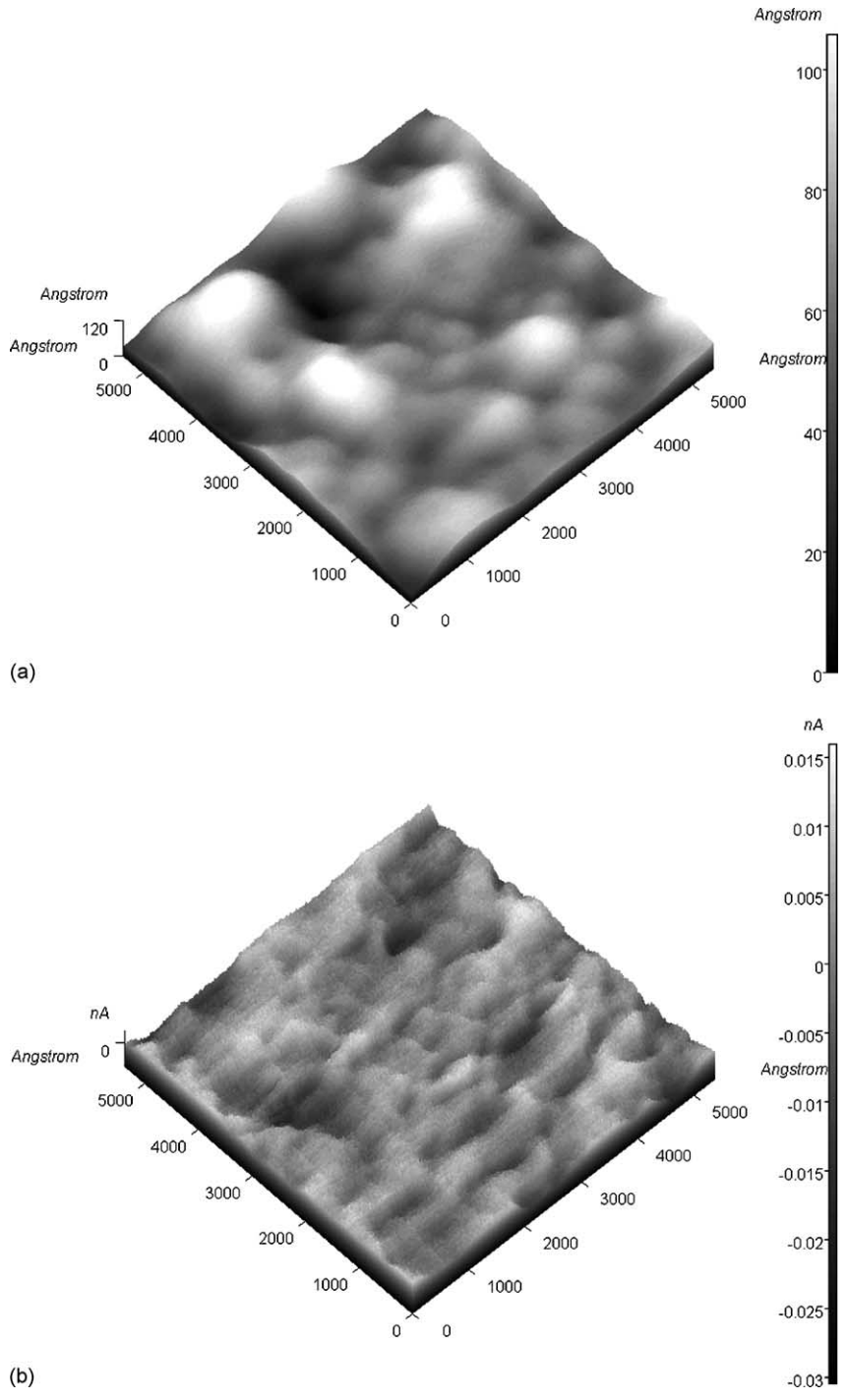

Fig. 13. (a) Surface topography and (b) force modulation image of 21 alternate layers of Gd_2O_3 and SiO_2 355 nm reflection filter for Nd:Yag-III laser recorded just after the development (October 2001).

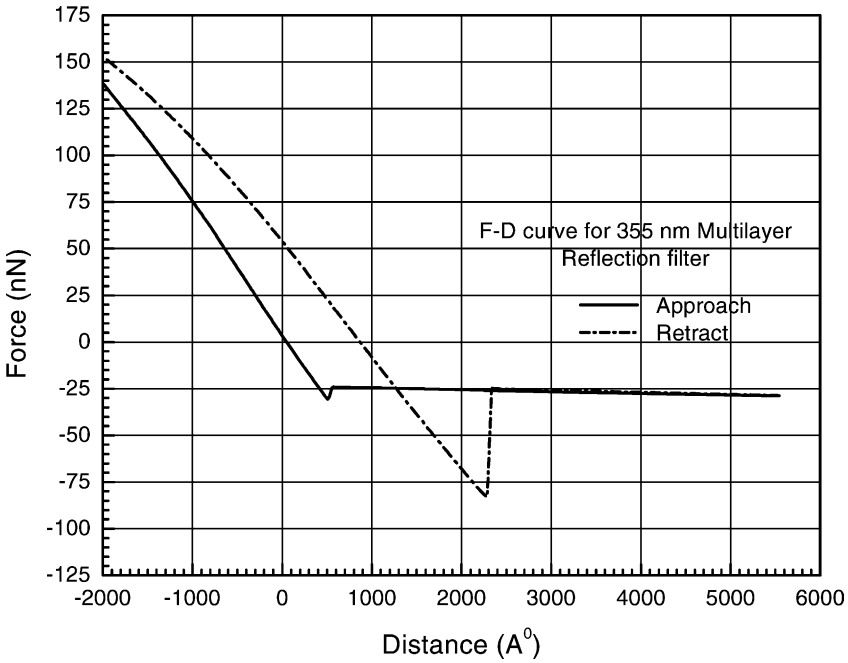

Fig. 14. Force vs. distance curve for the 21-layer 355 nm reflection filter.

layers. The corresponding force modulation image is depicted in Fig. 13b. This image indicates that the elasticity is uniform all over the sample surface of the multilayer. This clearly indicates that the Gd_2O_3 films with optimized process parameters can lead to stable multilayer structure when it is combined with the compatible and process optimized SiO_2 films. The force versus distance curve for the sample multilayer is plotted in Fig. 14. The adhesion force and the slope values are computed to be 57.96 nN and 0.06129 nN/Å, respectively. Although the adhesion force is less than that of 248 nm reflection filters, it is at least comparable to the component single layer thin films. However, the relative stiffness (slope) is slightly higher than single layer films indicating an improvement in the structural parameter. All these studies have pointed out that the 248 nm multilayer is more stable than 355 nm filter. A possible explanation of such a better result may be the improved structural stability attainment due to an optimum number of layers in the former multilayer. In addition, the 248 nm filter has shown smoother surface topography in comparison to the 355 nm filter as shown in Table 2.

6.4. Spectrophotometric measurements

The spectral characteristics of these two filters have been recorded just after the developments (October 2001) and also after a time interval of 10 months (July 2002). Shimadzu spectrophotometer system model UV310PC has been used for these spectral measurements. Fig. 15 depicts the spectral characteristics of 248 and 355 nm filter recorded at two different point of time. Both the filters have shown excellent spectral stabilities with a relatively better value for the 248 nm reflector.

6.5. Correlation of spectral stability and microstructural measurements

Spectral stability of developed multilayer can very be well correlated with viscoelasticity measurements. The filter developed for KrF (248 nm) laser application showed relatively better stability than the filter for Nd:YAG-III (355 nm). The corresponding topography and viscoelasticity measurements recorded after 10 months have been presented in Figs. 16 and 17. In Fig. 16a and b the topography and the corresponding

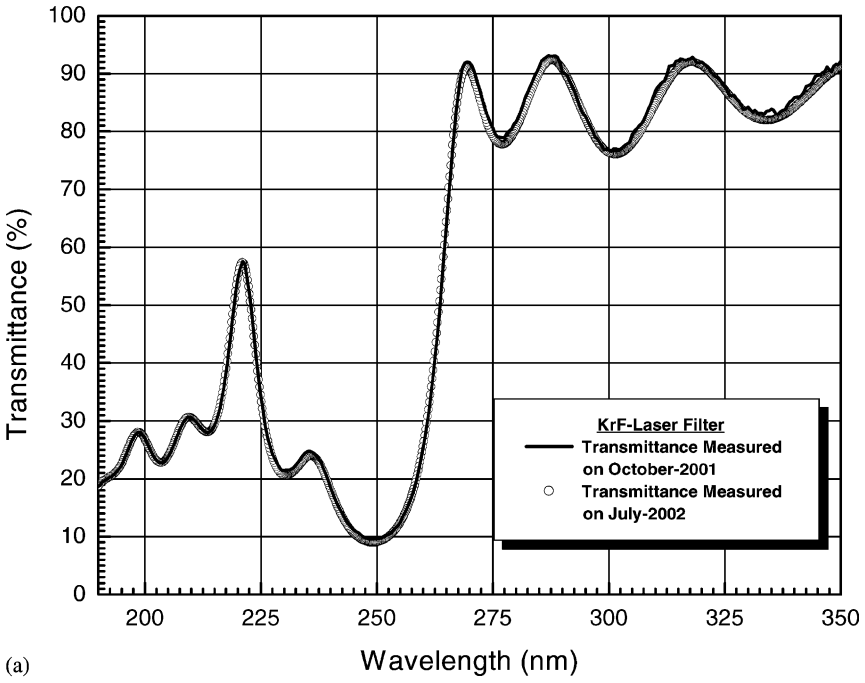

(a)

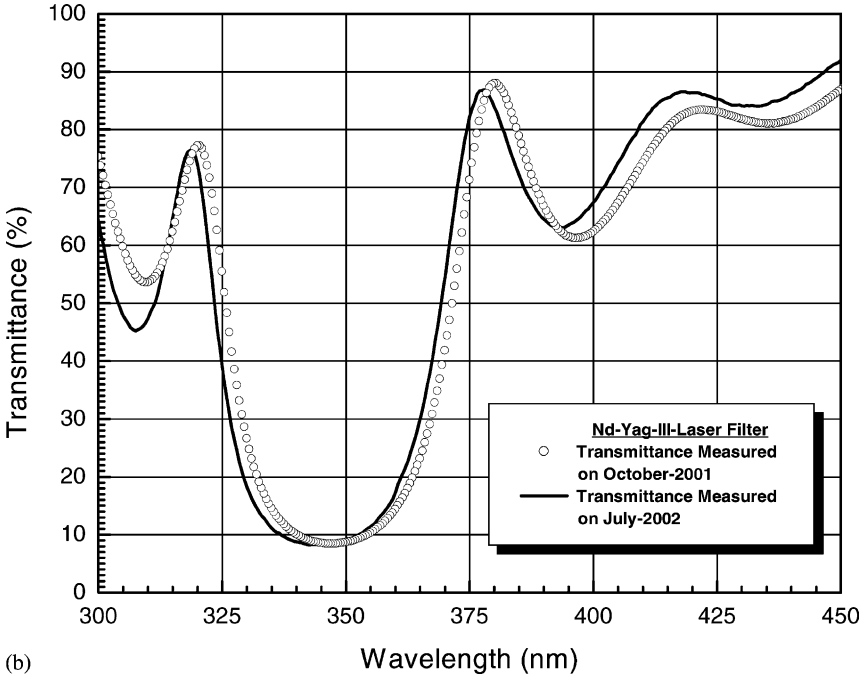

(b)

Fig. 15. Spectral transmittance characteristics of (a) 248 nm and (b) 355 nm reflection filters measured in October 2001 and June 2002; i.e. at a time interval of ∼10 months.

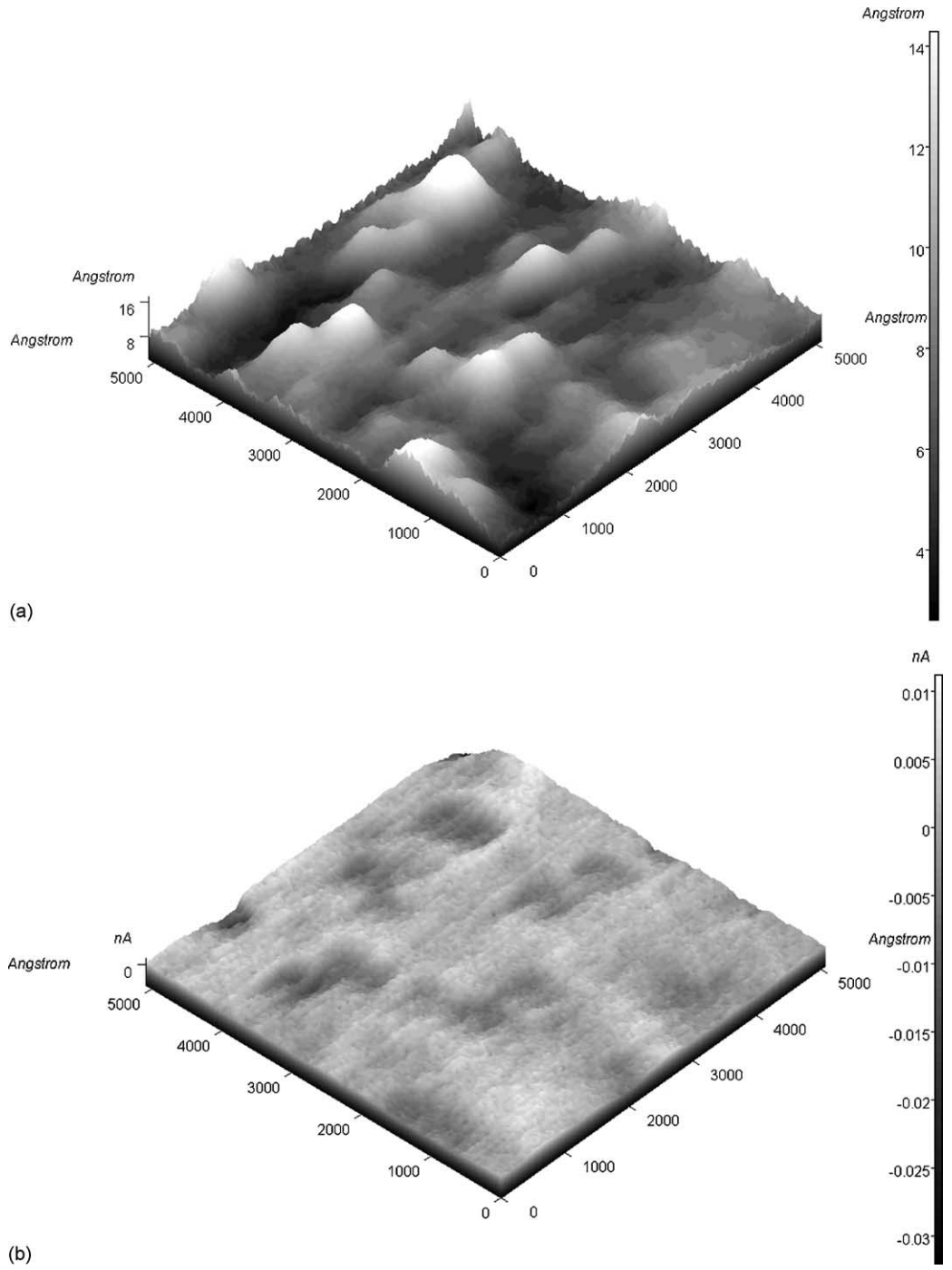

Fig. 16. (a) Surface topography and (b) force modulation image of 25 alternate layers of Gd_2O_3 and SiO_2 248 nm reflection filter recorded after 10 months (June 2002).

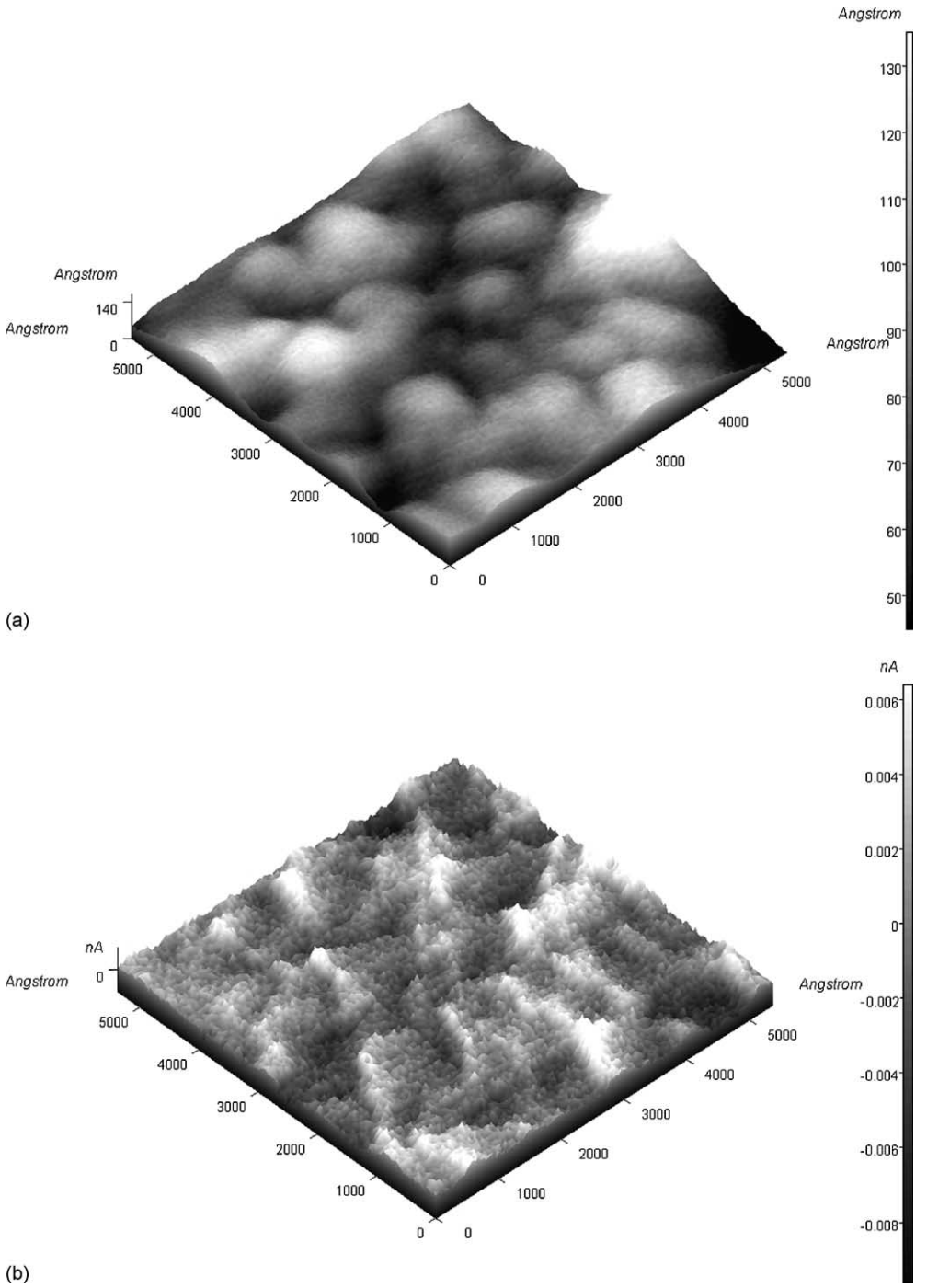

Fig. 17. (a) Surface topography and (b) force modulation image of 21 alternate layers of Gd_2O_3 and SiO_2 355 nm reflection filter recorded after 10 months (June 2002).

viscoelasticity of 248 nm reflecting filters are depicted. Similarly, in Fig. 17a and b the results for 355 nm filter have shown. These measurements indicated that the 355 nm filter have shown a bit more deviation in the subsequent AFM measurements. This is the reason that this 355 nm filter has shown a relatively more shift in the spectral characteristic in comparison to the 248 nm filter.

However, both the filters have shown smooth topographies and uniform elasticity, which is evident from the topographic and force modulation images. In addition, these filters have exhibited good adhesion force and better relative stiffness, which are computed from force–distance curve. These measurements indicate that Gd_2O_3 films deposited under optimized process parameters have superior compatibility with SiO_2 films for developing multilayer optical coatings. It is interesting to note that 248 nm filter have shown much better visco elasticity property and adhesion in comparison to the 355 nm filter. Such an observation has been reflected in the spectrophotometric spectral stability measurements, which have shown almost no spectral shift in the 248 nm filter and a small spectral change in 355 nm filter.

7. Conclusion

Single and multilayer thin films have been prepared using Gd_2O_3 and SiO_2 thin films. These thin films have been studied for their structural stability, using surface topographic and viscoelasticity measurements (force modulation and force–distance measurements). The superior viscoelasticity, high adhesion force, better relative stiffness have made the Gd_2O_3 material to be good compatible candidate for making stable multilayers with SiO_2 film. Better viscoelasticity property has been observed for 248 nm filter, which uses relatively more number of layers (25 layers) than the 355 nm filter (21 layers). Spectral measurements have been recorded at two different point of time to identify the temporal spectral stability of two multilayer thin film filters fabricated for KrF (248 nm) and Nd:Yag-III (355 nm) lasers. These two filters are found to be quite stable by our spectrophotometric measurements with a relatively better result obtained for the 248 nm filter. Viscoelasticity measurements and force–distance AFM measurements have supported these observations. The improved result for 248 nm filter indicates that an appropriate number of layers in the multilayer structure can lead to a better structural stability.

References

[1] H.A. Macleod, Thin-Film Optical Filters, IOP Publishing, Bristol, 2001.
[2] P. Baumeister, Appl. Optics 40 (2001) 1132.
[3] E.P. O'Reilly, A.R. Adams, IEEE J. Quantum Electron. 30 (1994) 366.
[4] A.G. Cullis, D.J. Robbins, A.J. Pidduck, P.W. Smith, J. Cryst. Growth 123 (1992) 333.
[5] J.M. Millunchick, T.D. Twesten, D.M. Follenstaedt, S.R. Lee, E.D. Jones, Y. Zhang, S.P. Ahrenkiel, A. Mascarenhas, Appl. Phys. Lett. 70 (1997) 1402.
[6] A. Ponchet, A. Rocher, J.Y. Emery, C. Starck, L. Goldgtein, J. Appl. Phys. 77 (1995) 1977.
[7] M.A. GrinFeld, Sov. Phys. Dikl. 31 (1986) 831.
[8] D.J. Srolovitz, Acta Metall. Mater. 37 (1989) 621.
[9] D.J. Eaglesham, M. Cerullo, Phys. Rev. Lett. 64 (1990) 1943.
[10] W.H. Yang, D.J. Srolovitz, J. Mech. Phys. Solids 42 (1994) 1551.
[11] D.E. Jesson, S.J. Pennycook, J.M. Baribeau, D.C. Houghton, Phys. Rev. Lett. 71 (1993) 1744.
[12] N. Sridhar, J.M. Rickman, D.J. Srolovitz, Microstructural stability of stressed lamellar and fiber composites, Acta Mater. 45 (1997) 2715.
[13] N. Sridhar, J.M. Rickman, D.J. Srolovitz, Multilayer film stability, J. Appl. Phys. 82 (1997) 4852.
[14] A.A. Dakhel, J. Optics A: Pure Appl. Optics 3 (2001) 452.
[15] S. Hosaka, H. Koyanagi, A. Kikukawa, M. Miyamoto, K. Nakamura, K. Etoh, Jvac. Sci. Technol. B 15 (1997) 788.
[16] H.-Y. Nie, M. Motomatsu, W. Mizutani, H. Tokumoto, Thin Solid Films 273 (1996) 143.